

28 Apr 1981, 2:00 pm - 5:00 pm

Passive Earth Pressure During Earthquakes

H. Matsuzawa
Nagoya University, Nagoya, Japan

A. Matsumura
Taisel Corporation, Tokyo, Japan

Follow this and additional works at: <https://scholarsmine.mst.edu/icrageesd>



Part of the [Geotechnical Engineering Commons](#)

Recommended Citation

Matsuzawa, H. and Matsumura, A., "Passive Earth Pressure During Earthquakes" (1981). *International Conferences on Recent Advances in Geotechnical Earthquake Engineering and Soil Dynamics*. 4. <https://scholarsmine.mst.edu/icrageesd/01icrageesd/session03/4>



This work is licensed under a [Creative Commons Attribution-Noncommercial-No Derivative Works 4.0 License](#).

This Article - Conference proceedings is brought to you for free and open access by Scholars' Mine. It has been accepted for inclusion in International Conferences on Recent Advances in Geotechnical Earthquake Engineering and Soil Dynamics by an authorized administrator of Scholars' Mine. This work is protected by U. S. Copyright Law. Unauthorized use including reproduction for redistribution requires the permission of the copyright holder. For more information, please contact scholarsmine@mst.edu.



Passive Earth Pressure During Earthquakes

H. Matsuzawa, Associate Professor

Dept. of Geotechnical Engineering, Nagoya University, Nagoya, Japan

A. Matsumura, Engineer

Taisei Corporation, Dept. of Design and Construction, Tokyo, Japan

SYNOPSIS In order to investigate characteristics of the passive earth pressure during earthquakes against the front face of the part of sheet pile walls driven into the ground, dynamic earth pressure tests were performed by using a large scale oscillating soil bin. A movable wall from which inertial effects were eliminated was used in this study. The wall was moved toward sand filled in the bin during oscillation. The angle ϕ_m deduced by inserting the observed peak wall load and wall friction angle at the maximum inertia force into the logarithmic spiral method was coincided with that of the static condition. The change in the wall friction angle induced by oscillation should not be neglected in an estimation of passive earth pressure during earthquake.

INTRODUCTION

Most studies of earth pressure during earthquakes have been devoted to the active states. In the earthquake resistant design of retaining structures such as sheet pile walls, however, it is necessary to estimate the passive resistances during earthquakes against the front face of the part of the wall driven into the ground.

Mononobe (1924) modified Coulomb's solution to estimate the active and passive earth pressure during earthquakes. Recently another analytical solutions concerning the passive earth pressure on the wall during earthquakes were given by Ichihara et al. (1973) and Jakovlev (1977) based on Sokolovski's method. Ichihara et al., in their report, also modified the logarithmic spiral method to estimate the passive earth pressure during earthquakes and concluded that the solutions based on Sokolovski's method and the logarithmic spiral method are almost the same as each other in the case of $\delta=2/3\cdot\phi$ and $\alpha_1=-30^\circ$, where α_1 is the inclination angle of the front face of the wall against the vertical plane. These analytical solutions were derived from those in the static states by the addition of rigid body forces proportional to the ground acceleration respectively. These solutions neglected the inertial effects on the retaining structure itself and the resultant force of earth pressure acts $H/3$ above the base of the wall, where H is the height of the wall. According to these analytical solutions, the magnitudes of the passive earth pressure against the wall during earthquakes decrease as the ground acceleration increases. No studies, however, have been made so far to check the availability of these solutions experimentally.

This paper describes an experimental study on passive earth pressure during an earthquake using dry sand fill against a movable wall from which inertial effects had been eliminated.

DESCRIPTION OF TESTING APPARATUS

Oscillating Soil Bin

A large scale soil bin with a movable wall, as shown in Fig. 1, was used in this study. The inside dimensions of the bin were 230 cm in length, 200 cm in width and 75 cm in depth. The movable wall, as shown in Fig. 2, was installed at a distance of 30 cm inward from one end of the bin. In order to reduce the bottom effects of the bin, a space of 25 cm was left between the bottom plate and the lower end of the movable wall. The side walls of the bin were formed of 2 cm thick steel plates. In order to observe deformation of the sand filled in the bin and to reduce side friction between the inside surface of the side walls and the sand, one of the side walls had two 1.5 cm-thick glass windows each of 60 cm by 80 cm and the other was covered with 0.8 cm thick glass plates.

The soil bin was installed in a framework and supported horizontally by six plate springs which fixed to the framework, as shown in Fig. 1,



Fig. 1 Soil bin supported by plate springs

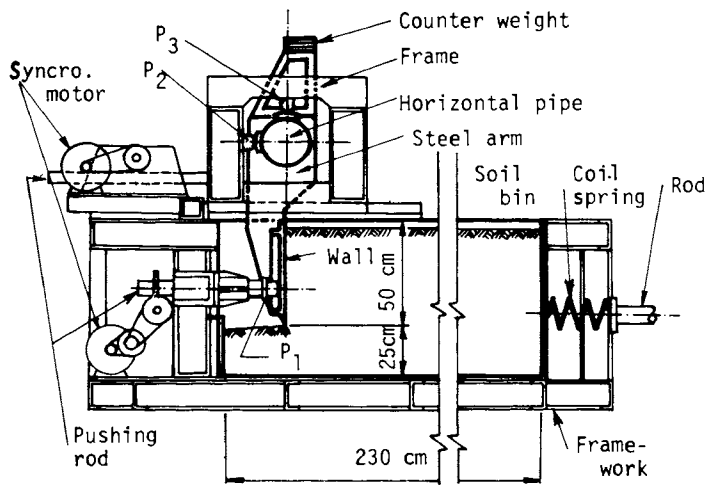


Fig. 2 Schematic diagram showing the section of soil bin

and the bin was forced to oscillate horizontally by two rods which pushed through soft coil springs. The rods were moved through a crank shaft and pulleys by a 15 h.p. AC motor and the amplitude of movement and frequency of the rods was variable. The total weight of the bin and the movable wall was 108 kN. The bin containing dense dry sand 70 cm deep weighed 148 kN. The bin could be oscillated at a resonant state with a maximum acceleration of 500 gals and a frequency of 2.67 Hz.

The Movable Wall

The movable wall is 200 cm wide, 50 cm high and 2.5 cm thick and consisted of two separate sections each 100 cm wide, as shown in Fig. 3. Each section of the wall, which had been strengthened from the outside by using stiffeners, was made of cast duralumin and the inside surface was finished to a smooth plane. Each section of the wall was supported by a horizontal pipe through four steel arms and could rotate around the pipe, as shown in Fig. 3. Each horizontal pipe was supported by a rotal support and could rotate around the horizontal and vertical axis, x and z , through the center point of the rotal support, as shown in Fig. 3.

The self weight of each section of the wall was counterbalanced by a set of counter weights fixed to the horizontal pipe and to each section, as shown in Figs. 1 and 3. In this way, the pure dynamic earth pressure on each section could be measured during oscillation.

When the movable wall was subjected to the earth pressure due to the sand filled in the bin, each section of the wall was supported by the rotal support and two load transducers, P_1 and P_2 , in the horizontal direction, and by the rotal support and a load transducer, P_3 , in the vertical direction respectively. The rotal support and the two load transducers, P_2 and P_3 , were fixed to a frame on the top of the bin, as shown in Figs. 1 and 2, and the frame could be moved horizontally over the bin. When the load transducer, P_1 , and the frame were moved through the same distance horizontally, the wall moved parallel to its initial position. A specified movement of the load transducer P_1 and the frame on the bin was produced by rotating synchronous

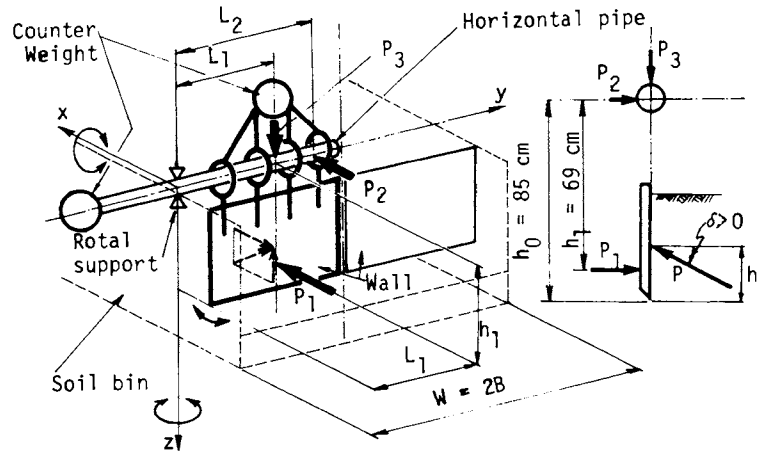


Fig. 3 Schematic diagram showing the method of measuring earth pressure (Details are illustrated for the left section only)

motor systems.

In order to prevent a rotating moment induced by friction between the inside surface of each section and the adjacent sand and by the toe shear force about the axis of the horizontal pipe, the inside surface of the movable wall was adjusted to coincide with the axis of the pipe and a steel knife edge was mounted on the base of the wall.

From the momentum equilibrium of forces around the axis of the horizontal pipe and the horizontal and vertical axis of the rotal support, we get the normal component of the resultant force of the earth pressure, $P \cos \delta$, the height of the point of application of the resultant force, h , and the coefficient of wall friction, $\tan \delta$, which is shown as follows;

$$P \cos \delta = P_1 + n P_2$$

$$h = h_0 - \frac{P_1 h_1}{P_1 + n P_2} \quad (1)$$

$$\tan \delta = \frac{P_3}{P_1 + n P_2}$$

where h_0 is the distance measured from the axis of the horizontal pipe to the toe of the wall ($h_0 = 85$ cm), h_1 is the distance measured from the axis of the horizontal pipe to the load transducer, P_1 ($h_1 = 69$ cm), n is a lever ratio ($= L_2/L_1$), as shown in Fig. 3, and P_1 , P_2 and P_3 are the measured forces of the load transducers, respectively. Assuming the linear distribution of earth pressure along the wall, the coefficient of earth pressure, K , is given as follow:

$$K = \frac{2P \cos \delta}{\gamma H^2 B} \quad (2)$$

where γ is the unit weight of the sand filled in the bin, H is the height of the wall and B is the width of each section of the wall.

DETAILS OF THE SAND USED IN THE TEST

Dry Toyoura sand was used in this study. The specific gravity of this sand, G_s , is 2.65, the maximum and minimum grain size and the effective size is respectively 0.25 mm, 0.105 mm and 0.16 mm, and the coefficient of uniformity is 1.65. The value of the internal friction under the plane strain condition, ϕ_p , of this sand of which the initial void ratios, e , are $0.677 \sim 0.698$, was estimated to 50° under the confining pressure of 9.8 kN/m^2 by using the next equation given by Ichihara and Matsuzawa (1973a).

$$\phi_p = 1.27\phi_T - 8.13 \text{ (degrees)} \quad (3)$$

where ϕ_T is the angle of internal friction determined by the triaxial compression test at the same void ratio and the same confining pressure.

TEST PROCEDURE

After the movable wall was adjusted to the vertical, the bin was filled with sand and compacted by vibrators to a depth of 70 cm. The height of the wall in contact with the sand was 45 cm. The sand was compacted in three stages at every 25 cm in depth. After compaction, the surface of the sand was levelled horizontally and the distance between the top of the bin and the surface of the sand was measured at several points. The value of average unit weight of the sand in the bin was calculated utilizing the total weight of the sand in the bin and its compacted volume. In each test the value of the average unit weight of the sand was between $15.3 \sim 15.5 \text{ kN/m}^3$ which corresponded to the void ratio of between $0.677 \sim 0.698$ and to the relative density of between $75.0 \sim 81.0 \%$. The soil bin was then oscillated at the resonant condition and the wall was moved toward the sand.

The acceleration of the bin, the loads at the three load transducers, P_1 , P_2 and P_3 , and the phases corresponding to the rotated angle of the pushing rods which were attached to the frame on the top of the bin and to the wall through the load transducer, P_1 , were recorded by a data recorder. The recorded phases were utilized to determine the wall displacement from its initial position.

RESULTS OF THE EXPERIMENT AND DISCUSSION

Variations of Oscillating Earth Pressure with Time

Fig. 4 shows the relationships of the acceleration of the soil bin, α , the coefficient of earth pressure, K , the relative height, h/H , of the resultant force of earth pressure and the coefficient of wall friction, $\tan \delta$, with time at near the peak wall load. It is obvious that each value of K , h/H and $\tan \delta$, oscillates as the bin oscillates and the wave phase of the relative height, h/H , of the point of application of the resultant force of earth pressure has about a 180-degree lag and that of the coefficient of wall friction, $\tan \delta$, has a 270-degree lag compared with the phase of the coefficient of earth pressure, K , respectively.

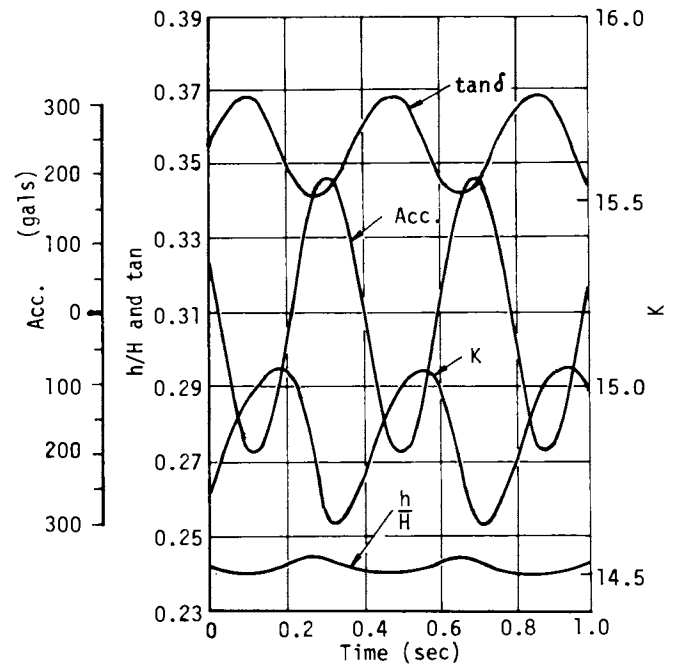


Fig. 4 Relationships of the acceleration of the bin, the coefficient of earth pressure, the relative height of the point of application of the resultant force and the coefficient of wall friction with time

Earth Pressure against the Wall

Figs. 5 and 6 show the values of the coefficient of earth pressure, K , the relative height, h/H , of the point of application of the resultant force of earth pressure and the coefficient of wall friction, $\tan \delta$, corresponding to the wall displacement, d , as typical examples under the static and dynamic conditions respectively. These figures also show the values of angle, ϕ_m , which were deduced by inserting the observed values of K and wall friction angle, δ , into the logarithmic spiral method developed by Ichihara et al. In Fig. 6 the solid lines show the values of K , h/H , $\tan \delta$ and ϕ_m at the maximum inertia force respectively and the dotted lines show those at the minimum inertia force, during oscillation. In this study, the maximum inertia force is defined as a condition during oscillation when the horizontal inertia force on the sand filled in the bin acts in the direction from the wall to the sand and its magnitude has reached the maximum, and the minimum inertia force as a inverse condition of the maximum inertia force. In the practical considerations, it is important to investigate characteristics of the earth pressure during oscillation.

As shown in Figs. 5 and 6, the initial values of the coefficient of wall friction, $\tan \delta$, were negative, i.e., the tangential component of the resultant force of earth pressure against the wall acts in a downward direction at the initial position of the wall. As the wall began to move toward the sand, the values of K and $\tan \delta$ increased remarkably. When the wall had moved about 10 mm from its initial position both in the static and dynamic conditions, the values of K reached their peak. The values of $\tan \delta$, however, were still increasing. For subsequent wall movement, the values of K decreased and the values of $\tan \delta$ increased to their ultimate values respec-

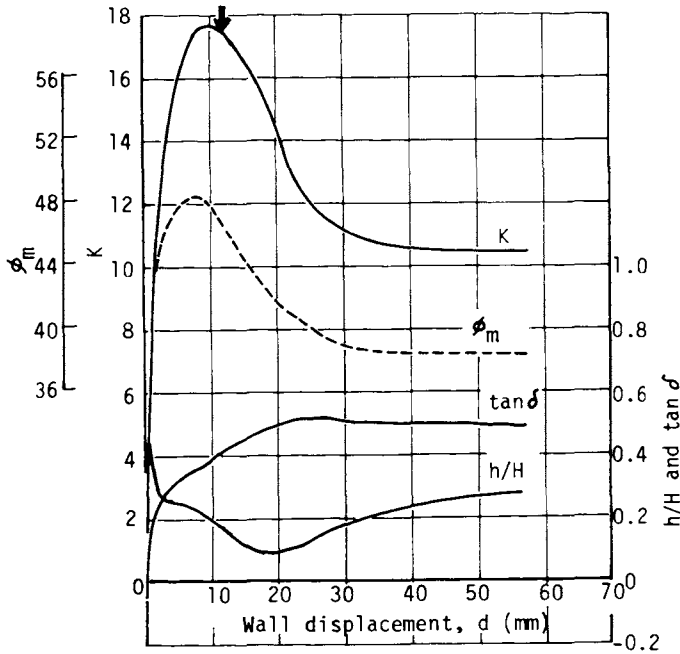


Fig. 5 Variation of the coefficient of earth pressure, the relative height of the point of application of the resultant force and the coefficient of wall friction corresponding to the wall displacement in the static condition

tively. The angle ϕ_m also increased in accordance with the wall movement and reached its peak value at a slightly small wall displacement than that of the peak wall loads, as shown in Figs. 5 and 6. After this the value of ϕ_m decreased for subsequent wall movement. In spite of the decrease of the value of ϕ_m , the coefficient of earth pressure, K , increased slightly and reached its peak value, because of the increase of the wall friction angle, δ . Arrows marked in Figs. 5 and 6 show the wall displacement where the sliding surface was observed at the surface of the sand. It was concluded from what we have described here that the failure of the sand mass along a sliding surface from the toe of the wall was induced at first and after this the slide between the wall and the adjacent sand occurred.

Effects of Side Friction

In two dimensional model test, it can be presumed that the forces on the wall measured by load transducers include the effects of side friction between the inside surfaces of the side walls of the bin and the sand. Rowe (1971) showed that the effects of side friction on the observed peak wall load are reduced by increasing the values of the width to height ratio, W/H , of the wall, and that the effects can be reduced considerably when the values of W/H are larger than 4.0. In the present study, the value of W/H is 4.4.

Fig. 7 shows the change in the distributions of earth pressure at the maximum inertia force corresponding to the acceleration of 420 gals, the distribution of which was measured by four pressure cells fixed to the wall. These pressure cells were near the center of the longitudinal direction of the wall. Therefore, it can be considered that the magnitude and distribution of the earth pressure indicated in this figure include only slight effects of side friction. Comparing the magnitude of the resultant forces

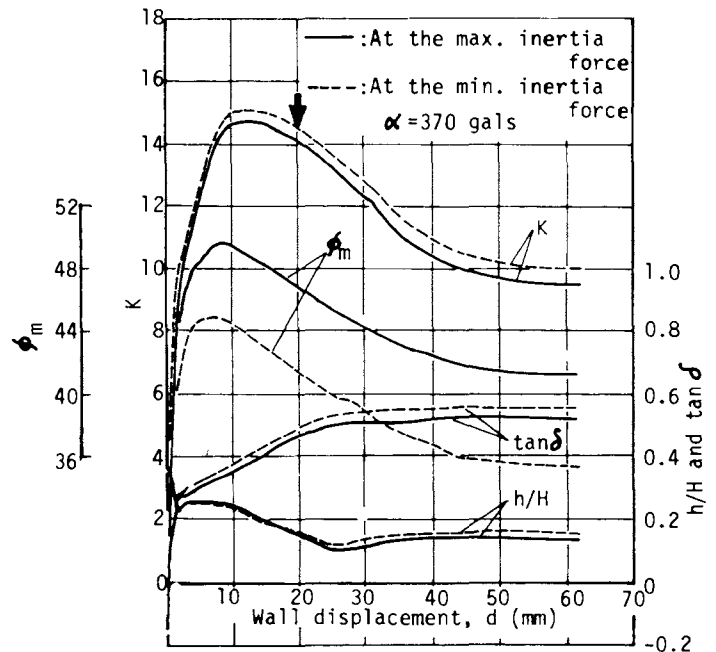


Fig. 6 Variation of the coefficient of earth pressure, the relative height of the point of application of the resultant force and the coefficient of wall friction corresponding to the wall displacement during oscillation

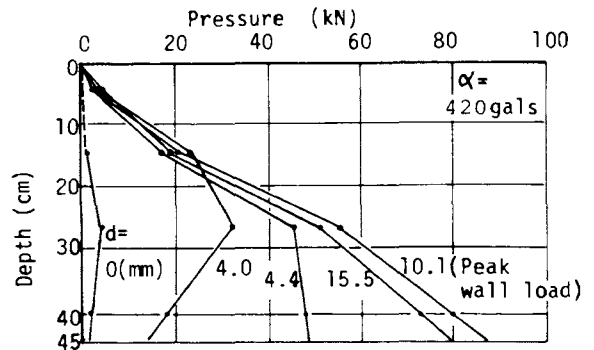


Fig. 7 Distribution of oscillating earth pressure along the wall at the maximum inertia force ($\alpha = 420$ gals)

of earth pressure measured by the load transducers with those obtained by integration of the pressure distribution diagrams, such as shown in Fig. 7, we found the former was only 8% larger than the latter before and at the peak wall load. However, it seemed that the relative height, h/H , of the point of application of the resultant force of earth pressure obtained by the load transducers was affected by side friction.

Characteristics of Earth Pressure at Peak Wall

Load

The values of wall displacement at the peak wall load, d_p , corresponding to the amplitude of acceleration of the bin, α_1 , are shown in Fig. 8. It is remarkable that the wall displacements which are required to induce the peak wall load during oscillation seem to be independent to the magnitude of the amplitude of acceleration, and that the values of d_p are about 9 mm ($d_p = 2.0 \times 10^{-2}$). Such a particular tendency as described here was also observed in the oscillating active

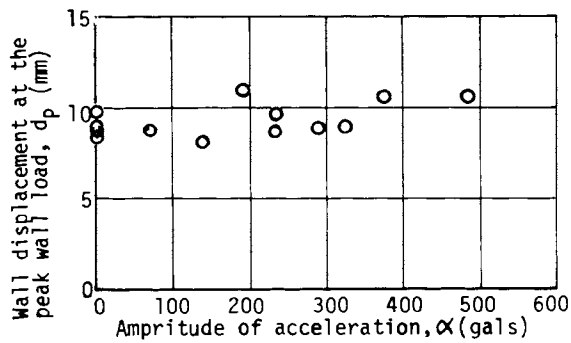


Fig. 8 Relationship between the wall displacement at the peak wall load and the amplitude of acceleration

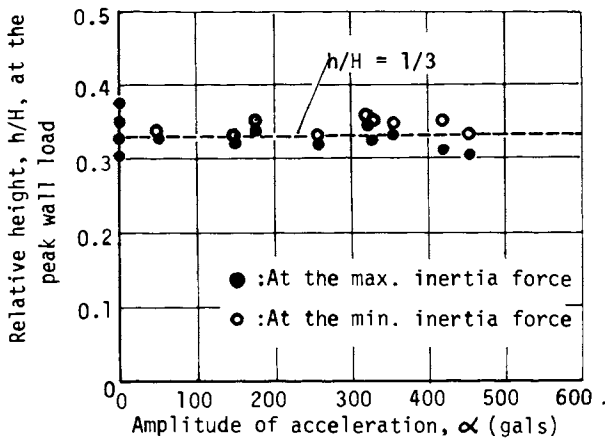


Fig. 9 Relative height of the point of application of the resultant force of earth pressure at the peak wall load corresponding to the amplitude of acceleration

earth pressure tests performed by Ichihara and Matsuzawa (1973b), i.e., regardless of the magnitude of the amplitude of acceleration, the relative displacement of the wall, d/H , which was required to induce the active state of dense back-fill sand was $(5.4 \sim 7.3) \times 10^{-4}$.

The values of relative height, h/H , of the point of application of the resultant force of earth pressure at the peak wall load, which are obtained from the pressure distribution diagrams such as shown in Fig. 7, against the amplitude of acceleration are shown in Fig. 9. It is obvious in this figure that the point of application of the resultant force oscillates with small amplitude but that the values of h/H are approximately a third for the horizontal translational wall movement.

Fig. 10 shows the values of the coefficient of earth pressure, K_p , in the static condition and that of K_{pE} both at the maximum and minimum inertia force in the dynamic condition respectively, corresponding to the amplitude of acceleration. Considerably large values of the coefficient of earth pressure K_p and K_{pE} , were measured, because a low model wall was used in this study. As shown in Fig. 10, the values of the coefficient of earth pressure, K_{pE} , at the maximum and minimum inertia force decreases in accordance with the amplitude of acceleration. However,

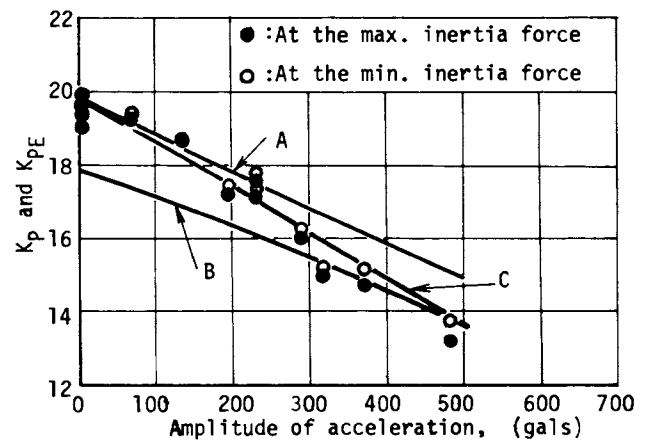


Fig. 10 Relationships between the coefficient of earth pressure and the amplitude of acceleration

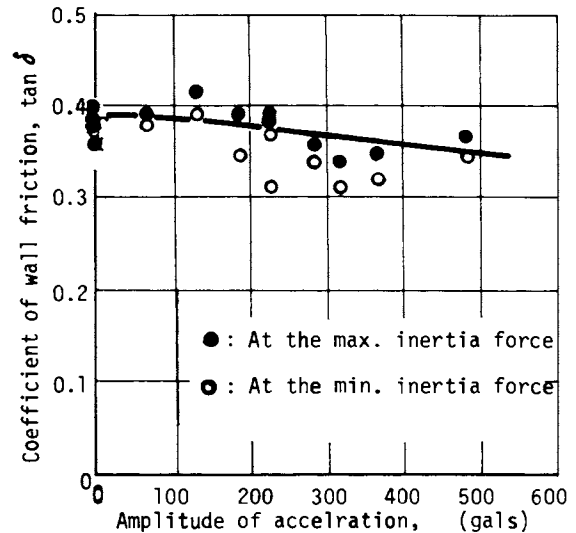


Fig. 11 The coefficient of wall friction at the peak wall load corresponding to the amplitude of acceleration

the amplitude of coefficient of earth pressure induced by the oscillation of the bin is small because of the very small amplitude vibratory rotation of the wall caused by the elastic deformation of the frame at the top of the bin. The variation of the coefficient of wall friction, $\tan \delta$, at the peak wall load corresponding to the amplitude of acceleration is shown in Fig. 11. As the amplitude of acceleration increases, the values of $\tan \delta$ decrease from 0.39 ($\delta = 21.3^\circ$) in the static condition to 0.35 ($\delta = 19.3^\circ$) at 500 gals. Fig. 12 shows the values of the angle at the peak wall load, ϕ_{mp} , which were deduced by inserting the observed values of K_{pE} and wall friction angle, δ , into the logarithmic spiral method for the maximum and minimum inertia force respectively. As shown in this figure, it is not clear whether the angle ϕ_{mp} at the maximum inertia force decreases in accordance with the amplitude of acceleration, but it can be considered that its value is 49.5° . For the minimum inertia force, however, the value of ϕ_{mp} decreased from 49.5° in the static condition to 42.8° at 500 gals.

Lines A and B, as indicated in Fig. 10, show the

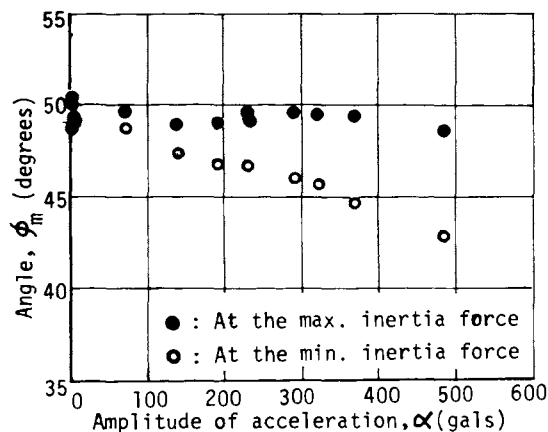


Fig. 12 The angle ϕ_{mp} corresponding to the amplitude of acceleration

theoretical passive earth pressure during earthquakes calculated by the logarithmic spiral method with the values of the angle of internal friction, ϕ , of 49.5° and the wall friction angles δ of 21.3° and 19.3° respectively. Line C shows the theoretical passive earth pressure calculated by using the same value of the angle of internal friction and the observed values of the angles of wall friction which are shown by a solid line in Fig. 11. Though the change in the wall friction angle, δ , induced by oscillation is only 2° between the static and dynamic conditions, as mentioned above, it can be concluded that the decrease of wall friction angle should be taken into account in the estimation of passive earth pressure during earthquakes based on the conventional analytical solutions.

CONCLUSIONS

Passive earth pressure during oscillation was measured by using a movable wall. Though the wall was counterbalanced to eliminate its inertial effects, the observed earth pressure on the wall seemed to be affected slightly by the elastic deformation of the frame on the top of the bin. From this study, the following conclusions could be made.

- 1) When the soil bin was oscillated horizontally, the resultant force of earth pressure on the wall, its point of application and the coefficient of wall friction oscillated. And, as the wall moved toward the sand, the passive failure was induced in the sand mass. However, it seemed that the failure of the sand mass along a sliding surface from the toe of the wall and along the surface of the wall did not occur simultaneously.
- 2) The relative wall displacements, d_p/H , at the peak wall load were not affected by oscillation, and their values were approximately equal to 2.0×10^{-2} for the 45 cm-high wall.
- 3) Both in the static and dynamic conditions, the earth pressures at the peak wall load were distributed approximately linearly along the wall, regardless of the amplitude of acceleration.

4) At the peak wall load during oscillation, the coefficient of earth pressure, K_{pE} , and the coefficient of wall friction, $\tan \delta$, decreased in accordance with the amplitude of acceleration. The amount of this decrease of wall friction angle from the static condition was only 2° at 500 gals. The value of the angle, ϕ_{mp} , at the maximum inertia force deduced by inserting the observed values of K_{pE} and wall friction angle δ into the logarithmic spiral method coincided with that of the static condition.

5) In an estimation of passive earth pressure during earthquakes which depends upon conventional methods, we can not neglect a decrease in the wall friction angle, δ , during oscillation.

ACKNOWLEDGEMENT

The authors wish to thank Mr. Yoshinobu Bitoh of Nakanihon Construction Consultant Co., Ltd. and Mr. Mitsuyoshi Yuge, a graduate student of Nagoya University for assisting in this experimental study. The authors are deeply in debt to Mr. G. Toff of Nagoya Institute of Technology for his help with the final English draft of this paper. The calculations of this study were made on a FACOM 230-75 Computer at Nagoya University Computer Center and this study was supported in 1978, 1979 and 1980 by Grants in Aid for Scientific Research from the Ministry of Education, Japan.

REFERENCES

- Ichihara, M. and Matsuzawa, H. (1970), "Experiments on Shearing Characteristics of Dry Sand under Plane Strain Condition and Axial Symmetric Condition", Proc. JSCE, No. 173, pp. 47-59. (in Japanese)
- Ichihara, M. and Matsuzawa, H. (1973), "Earth Pressure during Earthquake", Soils and Foundations, Journal of JSSMFE, Vol. 13, No. 4, pp. 75-86.
- Ichihara, M., Mori, N., Nakane, S. and Hirano, I. (1973), "Passive Earth Pressure Coefficient during Earthquake", Memoirs of the Faculty of Engineering, Nagoya University, Vol. 25, No. 2, pp. 129-179.
- Jakovlev, P. I. (1977), "Coefficients of Active and Passive Pressure on Retaining Walls under Seismic Conditions", Proc. 6th World Conf. on Earthquake Engineering, Vol. III, pp. 2356-2362, New Delhi.
- Mononobe, N. (1924), "Some Considerations of the Horizontal and Vertical Seismic Effects, and Miscellaneous Notes on Vibration", Journal of JSCE, Vol. 10, No. 5, pp. 1063-1094. (in Japanese)
- Rowe, P. W. (1971), "Large-scale laboratory model retaining wall apparatus", Stress Strain Behaviour of Soils, Proc. of the Roscoe Memorial Symp., Cambridge University, pp. 441-449.